A Comparison of Different Techniques to Quantify Moisture Content Profiles in Porous Building Materials

STAF ROELS,* JAN CARMELIET AND HUGO HENS
K.U.Leuven, Department of Civil Engineering
Kasteelpark Arenberg 51, B-3001 Leuven
Belgium

OLAF ADAN AND HAROLD BROCKEN
TNO Building and Construction Research
P.O. Box 49, 2600 AA Delft
The Netherlands

ROBERT CERNY AND ZBYSEK PAVLIK
Faculty of Civil Engineering
Department of Structural Mechanics
Czech Technical University
Thakurova 7, CZ-16629 Prague 6
Czech Republic

ARMIN T. ELLIS AND CHRISTOPHER HALL
Centre for Materials Science and Engineering
University of Edinburgh
The King's Buildings, Edinburgh EH9 3JL, UK

KUMAR KUMARAN
National Research Council Canada
Institute for Research in Construction
1200 Montreal Road, Ottawa ON K1A 0R6
Canada

*Author to whom correspondence should be addressed.

1097-1963/04/04 0261–16 $10.00/0 DOI: 10.1177/1097196304042117

LEO PEL
Department of Applied Physics
Eindhoven University of Technology
P.O. Box 513, 5600 MB Eindhoven
The Netherlands

RUDOLF PLAGGE
Institute of Building Climatology
University of Technology Dresden
Zellescher Weg 17, D-1069 Dresden
Germany

(Received September 10, 2003)

ABSTRACT: Several advanced non-destructive techniques are available to measure the evolution of content profiles with time, allowing the analysis of unsaturated flow and the determination of the moisture diffusivity of porous building materials. The reliability of six different techniques is investigated: the NMR-technique, the MRI-technique, the γ-ray attenuation technique, the capacitance method, the X-ray projection method and the TDR-technique. All of them were applied to measure the moisture content evolution during free uptake experiments on two building materials. Considering the limitations of some of the techniques, a good overall agreement is obtained. The work presented is an outcome of the EU-initiated HAMSTAD-project.

KEY WORDS: moisture content profiles, NMR, TDR, MRI, γ-ray, X-ray, capacitance method, round robin

INTRODUCTION

IN THE PAST analysis of moisture phenomena in porous building materials has been restricted to simple weighing of samples during wetting or drying. Obtaining moisture profiles was only possible in a destructive way. During the last decades, several advanced experimental techniques have been developed to determine transient moisture content profiles in a non-destructive way. Best-known in building physics are the γ-ray attenuation technique [3,9,11] and the NMR-technique [5,13]. However, several other techniques exist, such as the capacitance method [19], positron emission tomography [7] and neutron radiography [12,16]. Recently, Plagge et al. [15] applied the TDR-technique, originally used in soil sciences, to building materials. van Besien [22] and Roels et al. [17] presented the microfocus X-ray radiography, evolved from the well-known medical technique, for the analysis of moisture transport in porous building materials.

In this paper, six different techniques for analysing moisture flow in porous building materials are compared: the NMR- and MRI-technique, the γ-ray attenuation technique, the capacitance method, the X-ray projection method and the TDR-technique. In the framework of the EU-initiated HAMSTAD-project those six non-destructive techniques all measured the evolution of the moisture profiles during a capillary uptake experiment on two building materials: calcium silicate plate and fired clay brick. The question addressed was how well various laboratories employing different test methods can measure separate specimens from the same product batch.

MATERIALS INVESTIGATED

Calcium silicate plate and ceramic brick are two of the three materials chosen for laboratory testing in the round robin (samples of the same batch were sent to all participants) of the HAMSTAD-project [21].

The calcium silicate plate is a homogeneous, low-density board. It is mainly used as capillary active interior insulation, because of its high capillary-absorption coefficient and capillary moisture content. Table 1 summarises the basic hygric properties as measured on the material by the different partners of the HAMSTAD-project (see [18]). As can be seen the standard deviation of the measured properties is low.

The total open porosity of the second material, ceramic brick, is much lower. Contrary to the calcium silicate, where during an imbibition experiment, most of the pore space becomes filled with water, air becomes entrapped in a large part of the pore structure of the clay brick (see Table 1). Note also, that the standard deviation on the absorption coefficient and

Table 1. Mean and standard deviation of the basic hygric properties of calcium silicate plate and ceramic brick as determined in the round robin experimental work of the HAMSTAD-project. In brackets the number of samples is given.

	Calcium Silicate		Fired Clay Brick	
	Mean	**St Dev**	**Mean**	**St Dev**
ρ (kg/m^3)	267.57	2.92 (71)	2002.86	13.25 (76)
ρ_{mat} (kg/m^3)	2541.57	26.61 (71)	2628.68	7.34 (76)
Ψ_o (%)	89.47	0.13 (71)	23.81	0.56 (76)
w_{cap} (kg/m^3)	802.83	22.37 (62)	147.46	10.97 (64)
w_{sat} (kg/m^3)	894.7	1.34 (71)	238.1	5.55 (76)
A (kg/m^2 s$^{1/2}$)	1.223	0.085 (62)	0.160	0.028 (74)

capillary moisture content is relatively seen, much higher for the ceramic brick. This can be attributed to the nature of the material and the production process, which will result in a higher variability of the properties.

MEASUREMENT TECHNIQUES

Gamma-ray Attenuation Technique

In a gamma-ray experiment, a test sample is placed between the gamma-ray source and the detector of the gamma-ray equipment. A grid of vertical and horizontal co-ordinates defines the surface that faces the gamma-ray source. This arbitrarily divides the surface, and hence the specimen, into a two-dimensional array of columns and rows. The gamma-ray equipment can be focussed on any rectangular segment in such an array. At each segment of the specimen, the gamma-rays are emitted from the source and captured by the detector on the other side. Let the photons count last for a given period (e.g. 30 s). The test is first done on a dry specimen and I_0 denotes the count number for a given segment. Water is then added in a container at the bottom of the specimen to immerse the bottom surface only (approximately 3 mm). The time at which water touches the surface during filling is noted as "zero" time for the process. The temperature and level of water are held constant by circulating water from a temperature-controlled bath. As the water uptake proceeds, at regular intervals, gamma-rays are transmitted through each of the segments and emitted photons are analysed. If the count changes from I_0 to I and the average moisture concentration, c, in the segment is calculated from the equation:

$$(I/I_0) = e^{-\mu c x} \tag{1}$$

where μ is the mass attenuation coefficient for water that is characteristic for the energy of the incident gamma photons and x is the thickness of the specimen. The mass attenuation coefficient has to be determined for each gamma source and measuring equipment [11].

Thus scanning each segment gives an average value for the moisture content at a given interval and when all put together it results in the moisture distribution in the specimen as a function of time. The interval between each set of scanning steps depends on the rate of moisture movement in the specimen. The interval varies between 1 h and 24 h for common building materials.

X-ray Projection Method

The X-ray technique allows visualising in a non-destructive way, the interior of non-transparent objects, like porous building materials. For this purpose, the object is illuminated with X-rays and the change in transmitted X-ray intensity is measured. The HAMSTAD-experiments were performed on an AEA microfocus CT with an X-ray source energy up to 160 keV. The detector is a CCD 12-bit camera (4096 intensity levels). The intensity levels, I, are visualised as greyscales. The real-time images are digitised and imported by a Tomahawk image acquisition card into the PC. To reduce the noise, several projections taken at the same time are averaged. Acquiring an image by averaging 256 frames takes a little more than 10 s. The reconstructed greyscale images are 1024×1024 pixels.

For the water uptake experiments, an oven dry sample is placed in the X-ray apparatus, on a recipient, which can be filled with water. First, an X-ray image of the oven dry sample is taken. Then water is poured into the recipient. Images are now taken at regular time steps while the water is being taken up by the sample. Assuming monochromatic X-rays, the relationship between the intensity of the incident and attenuated X-rays (I_0 and I respectively) is expressed by Beer's law and the transmitted X-ray energy of the dry and wet sample can be written as:

$$I_{\text{dry}} = I_0 \exp(-\mu d) \tag{2}$$

$$I_{\text{wet}} = I_0 \exp(-\mu d - \mu_w d_w) \tag{3}$$

with μ and μ_w the attenuation coefficients of sample and water respectively, and d the thickness of the sample. d_w has to be read as the thickness of a fictitious water layer in agreement with the water content in the material. Defining the moisture content $w\,(\text{kg/m}^3)$ as:

$$w = \frac{\rho_w V_w}{V} = \frac{\rho_w d_w}{d} \tag{4}$$

Equation (4) can be rewritten as:

$$w = -\frac{\rho_w}{\mu_w d} \ln\left(\frac{I_{\text{wet}}}{I_{\text{dry}}}\right) \tag{5}$$

So by logarithmically subtracting the reference image of the dry sample from the images of the wet sample, the moisture content at each position can be quantified. Note that the attenuation coefficient depends on the density

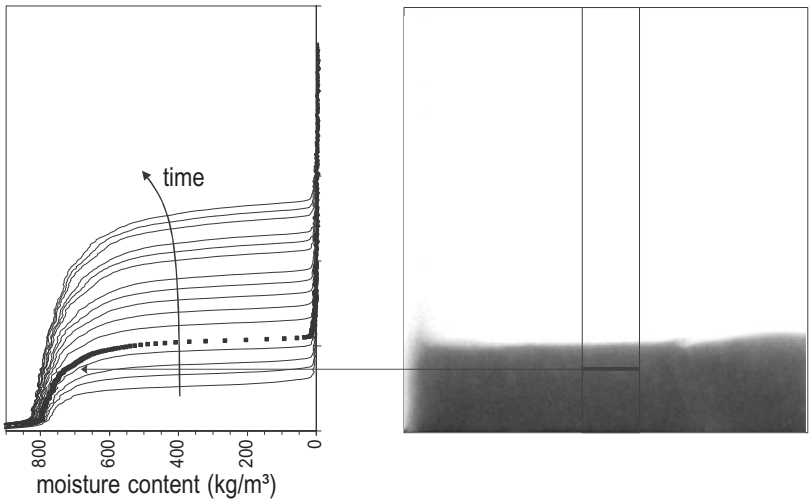

Figure 1. *Subsequent moisture profiles for calcium silicate plate determined from two-dimensional quantitative moisture profile images (right) as obtained by the X-ray projection method in a free uptake experiment.*

and atomic number of the material and the used X-ray energy. This makes it possible to determine for each material an optimal sample thickness to improve the resolution [22]. This optimal sample thickness, corresponding to an X-ray energy of 85 keV, is situated between 3 and 10 cm for calcium silicate plate and between 1 and 2 cm for the fired clay brick. For calcium silicate, a sample of 70×60 mm with a thickness of 30 mm is used. The overall dimensions of the fired clay brick sample were $50 \times 50 \times 14\,\text{mm}^3$. The corresponding resolution R_w is respectively $0.8\,\text{kg/m}^3$ and $3.2\,\text{kg/m}^3$. To increase the test precision, at each step in time, the moisture profile is determined as the average of a band width of 20 pixels in the middle of the image and perpendicular to the moisture front (see Figure 1).

NMR-technique

NMR is a magnetic resonance technique, where the resonance condition for the nuclei is given by:

$$f = \gamma B_0 \tag{6}$$

In this equation f is the resonance frequency, γ the so-called gyromagnetic ratio and B_0 the externally applied static magnetic field. Because each type of nucleus has a specific value of γ, the method can be made sensitive to only hydrogen and therefore to water. When a known magnetic field gradient is

applied, the resonance condition will depend on the spatial position of the nuclei. The NMR measurements reported in this paper were performed using a so-called spin-echo technique. Assuming a single exponential decay, the magnitude of a NMR spin-echo signal is given by:

$$S \sim \rho[1-\exp(-TR/T_1)]\exp(-TE/T_2) \tag{7}$$

where ρ is the proton density, T_1 the spin-lattice (longitudinal) relaxation time, TR the repetition time of the spin-echo experiment, T_2 the spin–spin (transverse) relaxation time, and TE the spin-echo time. This equation is valid if $T_1 \gg T_2$. As can be seen from Equation (7), small T_2 values lead to a decrease of the spin-echo signal whereas, on the other hand, small T_1 values are preferred, as this parameter limits the repetition time (usually $TR \approx 4\,T_1$).

However, in many common porous building materials, like fired-clay brick, usually large amounts of paramagnetic ions (e.g. Fe) are present. This complicates the NMR measurements by two effects. First, the relaxation time T_2 will be drastically decreased by paramagnetic centres at the surface of the pores. Secondly, due to the difference of the magnetic susceptibility of water and the porous material, local field gradients will be induced, which broaden the resonance line and thereby limit the spatial resolution. Therefore, the moisture transport of these materials was studied using an NMR apparatus, especially designed for this purpose [10,13]. This apparatus uses a conventional iron-cored electromagnet, generating a field of 0.7 T, corresponding to a hydrogen resonance frequency of 33 MHz. Home-built Anderson gradient coils were employed, yielding magnetic field gradients in one direction up to 0.3 T/m. With these gradients the one-dimensional resolution is of the order of 1.0 mm for the materials investigated. The apparatus is designed such that quantitative measurements can be performed. Therefore a specially designed Faraday shield is placed between the RF coil and the sample, to suppress the effects of changes of the dielectric permittivity by variations of the moisture content. The samples used are cylindrical rods with a diameter of 20 mm and a length up to 200 mm. In order to measure a moisture profile, the sample is moved through the NMR apparatus with the help of step motor.

MRI-technique

The MRI technique used is a variant of the preceding method, in which liquid-state proton density (and hence water content density) within the sample is measured using a radiofrequency pulse sequence known as SPRITE [1,8]. This is a *single-point imaging* technique, which minimises

the effects arising from the short spin relaxation times and variations of magnetic susceptibility within heterogeneous porous materials such as brick and concrete mentioned previously.

The MRI experiments were carried out using a 2.4 T, 32 cm i.d. horizontal bore superconducting magnet system. Spiral-SPRITE measurements were performed at 99.3 MHz using a phase encode time, t_p, of 40 μs, a recovery time, TR, of 2 ms, an rf flip angle, α, of 4°, 2564 k-space points per spiral and a delay between successive spirals of 5 s. The maximum gradient strength was 22 Gauss/cm, with a field of view of 8 cm × 8 cm. Spiral k-space data were transformed to a 64 × 64 Cartesian grid, giving a nominal image resolution of 1.3 mm. To image water uptake in the calcium silicate, a single scan was acquired in 10 s. The ceramic brick required 4 scans, taking 40 s to image. Cylindrical samples of ceramic brick and calcium silicate, 36 mm in diameter and 40 mm in length, were prepared. Samples were first dried at 25°C and 50% relative humidity for 48 h. To achieve controlled water uptake, a specially designed sample holder provided a reservoir of water at zero hydraulic pressure at the end of the sample. From the calcium silicate, Spiral-SPRITE images were acquired every 10 s until the wetting front had progressed through the sample, typically 12–15 min. Images of the ceramic were collected every 40 s for 45 min. The field of view was 8 cm.

Capacitance Method

A block diagram of the capacitance device is shown in Figure 2. The low-voltage supply drives an oscillator of 400 kHz working frequency which has a constant output voltage feeding a circuit where the measuring capacitor (with the analyzed moisture sample as dielectric) is connected in series with a resistance. This resistance determines the voltage after rectifying which depends in a significant way on the moisture content in the dielectric. The

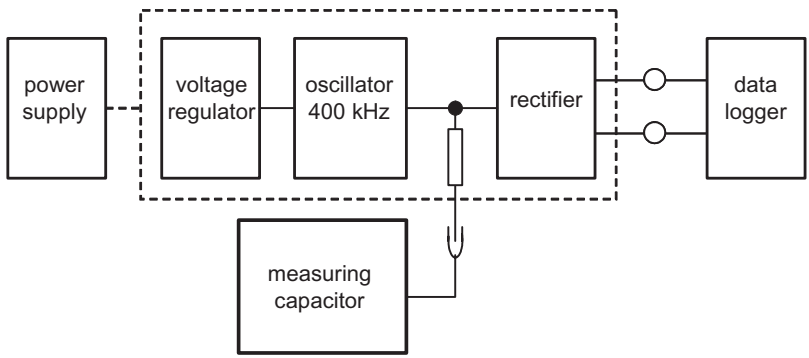

Figure 2. *Block diagram of the capacitance device.*

relationship between the moisture content of the specimen and the voltage measured on the resistance is determined by calibration. The measured voltage increases with increasing capacity. By a proper choice of the resistance it is possible to achieve that the dependence of the measured voltage on the capacity is linear in the range of approximately one or two orders of magnitude of the capacity. The voltage is recorded in specified time intervals by data logger.

The described capacitance moisture meter was equipped with electrodes in the form of parallel plates with dimensions of 20×40 mm. The moisture meter readings along the rod specimen were done every 5 mm in order to achieve certain space averaging of the results and reduce possible effects of inhomogeneity of the material.

The calibration curve of the capacitance moisture meter is usually for each material determined in advance using the gravimetric method. In this case, we have chosen another method and calibrated the device a posteriori using the moisture profile in the specimen after finishing the suction experiment, which was determined by the gravimetric method.

The overall dimensions of the specimen were $20 \times 40 \times 300$ mm. The edges were water and vapour proof insulated by thermally contractile PVC sheet to achieve a perfectly flat surface without air bubbles, which is necessary for a proper functioning of the measuring method (an even very thin air layer in series with the specimen can significantly affect the measured impedance).

TDR technique

The non-destructive TDR technique, known as cable radar, allows the automatic and continuous monitoring of volumetric water content in

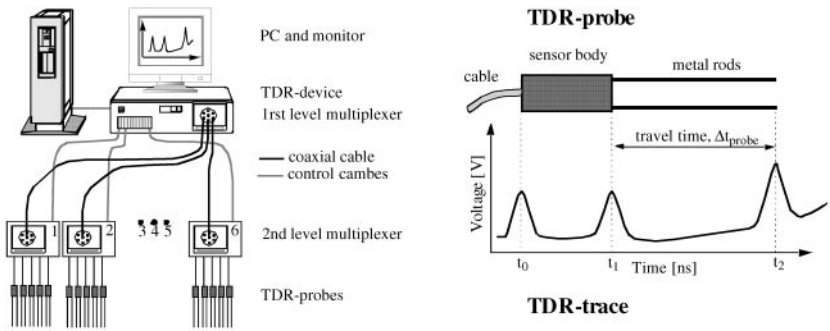

Figure 3. *Schematic view of the experimental set-up, able to monitor 36 miniaturized two-rods TDR-probes. A picture of the TDR trace and a reflectogram of the $\sin^n$-shaped electromagnetic pulse is presented. Note, having a rise time of 200ps, the technology applies frequencies between 50 MHz and 1.6 GHz.*

porous materials by means of dielectric measurements. A scheme of the TDR-system is shown in Figure 3, where also the basic components of the equipment are listed. The special measurement volume of a TDR-mini-probe is 2.8 cm^3 and can be approximated by a cylinder of 6 mm in diameter and 53 mm length.

For measurement, a TDR pulse is guided through the TDR probe, which is inserted in the respective material. If the travelling TDR pulse encounters changes in the electrical impedance surrounding the probe, part of the signal is reflected back towards the source. These reflections can be plotted as voltage as function of time, as given by the TDR-trace in Figure 3. The time of arrival and the magnitude of the reflected pulse are used to infer properties. The apparent dielectric constant, ε_a, can be determined using:

$$\sqrt{\varepsilon_a} = \frac{c}{2l}(t_2 - t_1) \tag{8}$$

where c is the velocity of the electro-magnetic wave in free space, $2.9979 \times 10^8\,ms^{-1}$, and l is the length of the embedded metal rods (m). t_1 and t_2 are the points of reflection (s), identifying the entrance and the end of the rods. Since the characteristic length, l, and t_1 of the probe are known by calibration using liquids of known dielectric constants, ε_a can be determined. The dielectric determination of the water content by TDR requires the knowledge of their relationship. Since the dielectric constant of free water is remarkably higher than of mineral materials or air, $\varepsilon_{water} \sim 81$, $\varepsilon_{brick} \sim 4$–$6$, $\varepsilon_{air} \sim 1$, the water content of the porous media can be obtained using a conversion or a calibration function.

Considering porous material to be a mixture of the phases; water, solid and air, the dielectric constant of the mixture can then be derived using the mixing law approach of Tinga et al. [20]:

$$\varepsilon_a = \left[\theta\varepsilon_w^{\beta} + (1-\phi)\varepsilon_s^{\beta} + (\phi-\theta)\varepsilon_a^{\beta}\right]^{1/\beta} \tag{9}$$

where the subscripts w, s and a are the dielectric constants of the phases water, solid material and air. θ and ϕ are the volumetric water content and the porosity and are used to define the volumetric fractions of the 3 phases. β corresponds to a geometry factor, accounting for the orientation of the imposed electrical field. Since β cannot be measured directly, the parameter is determined empirically using measured reference data and a least square minimization technique. More complex four-phase-models integrate the bound water fraction into the analysis [4,14] but require additional data and some assumption on the dielectric constant of bound water, leading to more fitting parameters and increasing model flexibility.

COMPARISON OF RESULTS

A direct comparison of the measured moisture profiles is difficult. Due to the characteristic features of each technique, the experimental data is obtained for different positions and different time steps. Furthermore, most of the techniques scan the specimen point wise. Therefore, comparing a profile at a certain time step would only be possible by an interpolation in the time domain. To overcome this problem, a Boltzmann transformation is applied to the experimental data. For each technique, the obtained moisture content versus distance profiles are plotted as a moisture content versus λ-profile, with

$$\lambda = xt^{-1/2} \tag{10}$$

If the Boltzmann-conditions are fulfilled (a constant boundary condition applied to a semi-infinite homogeneous medium that is initially at a uniform moisture content), all the measured moisture profiles should fall on a single λ-profile. Figure 4 compares the Boltzmann transformed experimental data of calcium silicate plate. Looking at the experimental data of one technique, the Boltzmann-transformation seems to hold very well. However, a systematic difference between the different techniques can be observed. In the case of the γ-ray attenuation technique, the uptake in the calcium silicate plate is so fast that only some limited points can be measured leading to less reliable results. For the other techniques the overall agreement is good.

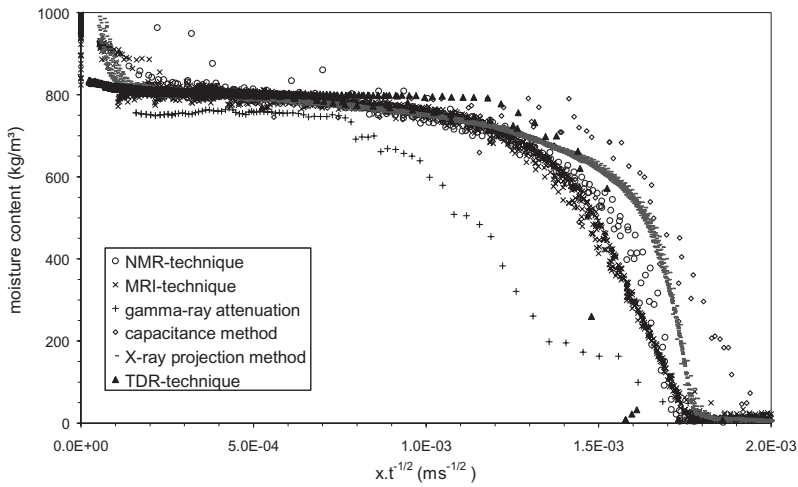

Figure 4. *All experimental data as obtained by the different techniques for calcium silicate plate plotted as moisture content vs.* λ $(\lambda = xt^{-1/2})$.

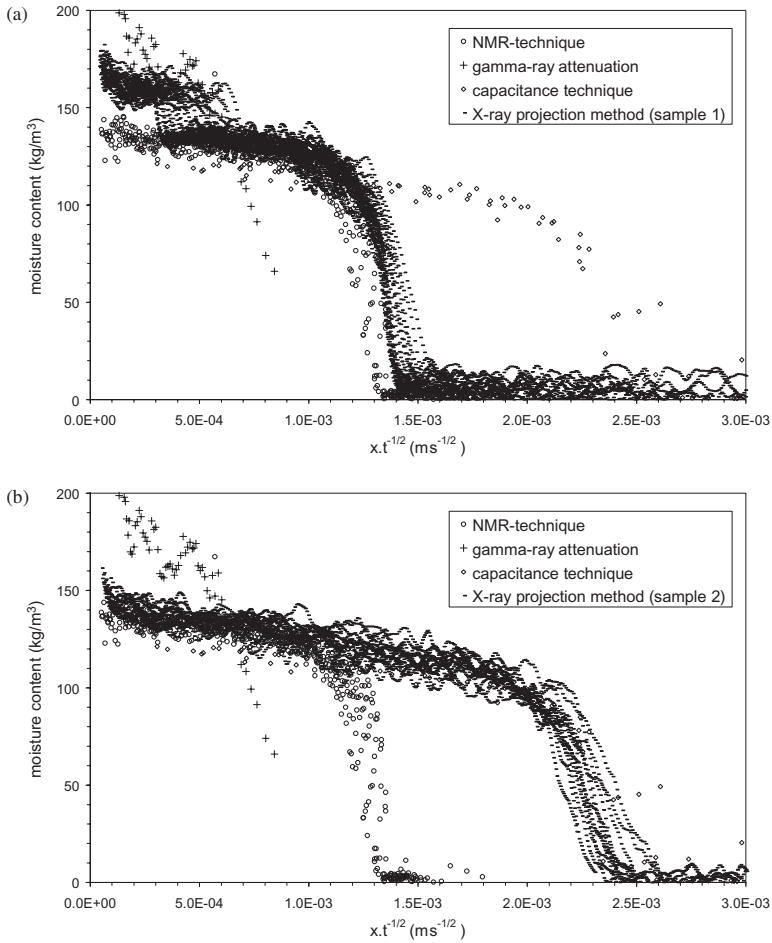

Figure 5. *All experimental data as obtained by the different techniques for fired clay brick plotted as moisture content vs. λ ($\lambda = xt^{-1/2}$). Figure (a) and (b) compare data as measured with the X-ray projection method of two specimens with distinct different absorption coefficient (sample 1: $A = 0.18\,kg/m^2s^{1/2}$, sample 2: $A = 0.26\,kg/m^2s^{1/2}$).*

A comparison of the experimental data obtained for fired clay brick is shown in Figure 5. At the moment, applying TDR to this kind of materials is still in an experimental stage, because of the contact problem between needle and material. Therefore, no results of TDR are shown for ceramic brick.

As could be expected, compared to the results on calcium silicate plate, the scatter on the experimental data is much higher. This is not only the fact within the data obtained with one technique, but also the deviation between the results of the different techniques is much higher. This, however, has

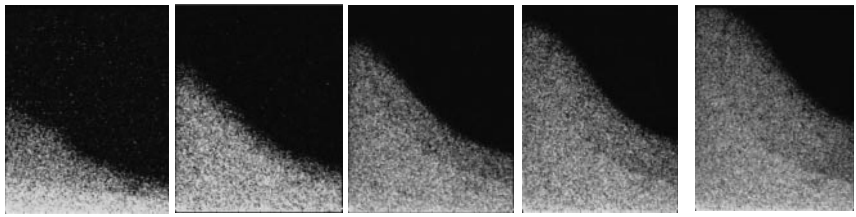

Figure 6. *Snapshots of the 2D moisture distribution as measured with the X-ray projection method during free water uptake in a brick specimen. The baseline of each image measures 50 mm. Imbibition from the bottom side. The inhomogeneity of the sample is clearly reflected in the moisture profile.*

more to do with the material investigated than with the applied technique. Figure 6, showing a 2D-image taken with the X-ray projection method, clearly illustrates the problem. Water uptake happens almost twice as fast on the left side of the specimen than on the right side. Note that the baseline of the image measures only 50 mm. Since most techniques measure on small specimen or scan one line within a specimen, this will result in considerable deviations between different measurements. As an example Figures 5a and 5b compare two samples, with distinct different absorption coefficient measured with the X-ray projection method. Where the results of the first sample ($A = 0.18\,\mathrm{kg/m^2s^{1/2}}$) correspond well with the results of the NMR-technique, the second sample ($A = 0.26\,\mathrm{kg/m^2s^{1/2}}$) is in close agreement with the data obtained with the capacitance method. This proves that the wide spread of results can be attributed to the inhomogeneity of the material as was demonstrated in Table 1. As a result the Boltzmann-condition of a semi-infinite homogeneous medium is not completely fulfilled, which will result in scatter on each λ-profile and deviations between the λ-profiles measured on different samples.

CONCLUDING REMARKS

Six different non-destructive techniques for the analysis of moisture flow in porous building materials were compared by scanning the moisture content profiles during free water uptake experiments on two building materials: calcium silicate plate and ceramic brick. Since most of the techniques scan the specimen point wise, a direct comparison of the measured profiles was not possible. Therefore, a Boltzmann-transformation was applied to the experimental data and the obtained λ-profiles were compared.

It was found that the results of the γ-ray attenuation technique deviate from the results obtained with the other techniques. This can be attributed

to the fact that the uptake process both in calcium silicate plate and in ceramic brick is so fast that only some limited points can be measured with this technique, leading to less reliable results. In the past, the technique showed to be much more reliable for materials with a lower absorption coefficient (see e.g. [3,11]).

The TDR-technique, adapted from soil sciences, was applicable for calcium silicate plate, a material where the needle can be installed through a pilot hole. Applying TDR to materials such as ceramic brick is still in an experimental stage, due to the installation problem of TDR-needles into hard materials.

The other four techniques: the NMR-technique, the MRI-technique, the capacitance method and the X-ray projection method, showed a good overall agreement. Looking at the results obtained on calcium silicate plate, the transformation of the measured data into a single λ-profile seems to hold very well. Between the different techniques, however, a small systematic difference was observed.

Compared to homogeneous calcium silicate plate, the transformed data of ceramic brick showed much more scatter. This gives evidence that the Boltzmann-condition of a semi-infinite homogeneous medium is not completely fulfilled. Furthermore it was found that different samples resulted in different λ-profiles. This can be attributed to the variability on the material properties and the fact that most techniques measure the moisture profiles on small samples.

That kind of scattered data, as presented in this paper, is normally used to derive the moisture diffusivity of the material. This determination is, however, not so straight forward. The derivation of the moisture diffusivity starting from this kind of experimental data was a subtask in the HAMSTAD-project and will be discussed in ([2]).

ACKNOWLEDGEMENTS

MRI-measurements were carried out at the MRI Center at the University of New Brunswick, Canada. We acknowledge the expert collaboration of Bruce Balcom, Bryce Macmillan and Igor Mastikhin in obtaining the data reported here.

The measurements with the X-ray radiography equipment were performed at the Department of Metallurgy and Materials Engineering of the K.U. Leuven. We would like to thank Martine Wevers for the fruitful collaboration.

REFERENCES

1. Balcom, B.J., MacGregor, R.P., Beyea, S.D., Green D.P., Armstrong, R.L. and Bremner, T.W. (1996). Single Point Ramped Imaging with T_1 Enhancement, *Journal of Magnetic Resonance*, **A123**: 131–134.
2. Carmeliet, J., Adan, O., Brocken, H., Cerny, R., Hall, C., Hens, H., Kumaran, K., Pavlik, Z., Pel, L., Plagge, R. and Roels, S. (2003). Determination of the Liquid Water Diffusivity from Transient Moisture Transfer Experiments, *Journal of Thermal Envelope and Building Science*, **27**(4): 277–305.
3. Descamp, F. (1997). *Continuum and Discrete Modelling of Isothermal Water and Air Transfer in Porous Media*, PhD Thesis, KULeuven, Leuven, Belgium.
4. Dobson, M.C., Ulaby, F.T., Hallikainen, M.T. and El-Rayes, M.A. (1985). Mikrowave Dielectric Behavior of Wet Soil, Part II: Dielectric Mixing Models, *IEEE Trans. Geosci. Remote Sensing*, GE-**23**(1): 35–46.
5. Gummerson, R.J., Hall, C., Hoff, W.D., Hawkes, R., Holland, G.N. and Moore, W.S. (1979). Unsaturated Water Flow within Porous Materials Observed by NMR Imaging, *Nature*, **281**: 56–57.
6. Hamilton, A. and Hall, C. (2002). Composition and Additional Characterisation of the Calcium Silicate Test Material, *HAMSTAD-Project*, *Work Document*, UoE2003-ho5, *University of Edinburgh*.
7. Hoff, W.D., Wilson, M.A., Benton, D.M., Hawkesworth, M.R., Parker, D. and Fowles, P. (1996). The Use of Positron Emisson Tomograhy to Monitor Unsaturated Flow within Porous Construction Materials, *Journal of Materials Science Letters*, **15**: 1101–1104.
8. Mastikhin, I.V., Mullally, H., MacMillan, B. and Balcom, B.J. (2002). Water Content Profiles with 1D Centric SPRITE Acquisition, *Journal of Magnetic Resonance*, **156**: 122–130.
9. Nielsen, A. (1972). Gamma-Ray Attenuation Used for Measuring the Moisture Content and Homogeneity of Porous Concrete, *Building Science*, **7**: 257–263.
10. Kopinga, K. and Pel, L. (1994). One Dimensional Scanning of Moisture in Porous Materials with NMR, *Rev. Sci. Instrum.*, **65**: 3673–3681.
11. Kumaran, M.K. and Bomberg, M. (1985). A Gamma-Spectrometer for Determination of Density Distribution and Moisture Distribution in Building Materials, In: *Proceedings of the International Symposium on Moisture and Humidity*, Washington DC, pp. 485–490.
12. Pel, L., Ketelaars, A.A.J., Odan, O.C.G. and Well, A.A. (1993). Determination of Moisture Diffusivity in Porous Media using Scanning Neutron Radiography, *International Journal of Heat and Mass Transfer*, **36**: 1261–1267.
13. Pel, L. (1995). *Moisture Transport in Porous Building Materials*, PhD Thesis, TU/e, Eindhoven, The Netherlands.
14. Plagge, R., Roth, C.H. and Renger, M. (1996). Dielectric Soil Water Content Determination Using Time-Domain Reflectometry (TDR), In: Kraszewski, A. (ed), *Workshop on Electromagnetic Wave Interaction with Water and Moist Substances at the 1996 IEEE Microwave Theory and Techniques Society International Microwave Symposium in San Francisco*, CA, pp. 59–62.
15. Plagge, R., Grunewald, J. and Haüpl, P. (1999). Application of Time Domain Reflectometry to Determine Water Content and Electrical Conductivity of Capillary Porous Media, In: *Proceedings of the 5th Symposium on Building Physics in the Nordic Countries*, pp. 337–344. Göteborg, Sweden.
16. Prazak, J., Tywoniak, J., Peterka, F. and Slonc, T. (1990). Description of Transport of Liquid in Porous Media – A Study Based on Neutron Radiography, *Int. J. Heat Mass Transfer*, **33**: 1105–1120.
17. Roels, S., Vandersteen, K. and Carmeliet, J. (2003a). Measuring and Simulating Moisture Uptake in a Fractured Porous Medium, *Advances in Water Resources*, **26**: 237–246.

18. Roels, S., Adan, O., Brocken, H., Carmeliet, J., Cerny, R., Hall, C., Hens, H., Kumaran, K., Pavlik, Z., Pel, L. and Plagge, R. (2003b). Interlaboratory Comparison of the Measurement of Basic Hygric Properties of Porous Building Materials, *Journal of Thermal Envelope and Building Science*, **27**(4): 307–325.
19. Semerak, P. and Cerny, R. (1997). Capacitance Method for Measuring Moisture Content of Building Materials, *Stavební obzor*, **6**: 102–103 (in Czech).
20. Tinga, W.R., Voss, W.A.G. and Blossey, D.F. (1973). Generalized Approach to Multi Phase Dielectric Mixture Theory, *Journal of Applied Physics*, 44: 3897–3902.
21. TNO (2003). HAMSTAD: Determination of Liquid Water Transfer Properties of Porous Building Materials and Development of Numerical Assessment Methods, Final Technical Report, European-project GRD1-1999-20007.
22. Van Besien, T., Roels, S. and Carmeliet, J. (2003). Analysis of Moisture Flow in Porous Materials using Microfocus X-ray Radiography, Submitted to *Physics D: Applied Physics*.